Robust Servomechanism LQR Comparison with Two- and Three-Loop Autopilot Designs

Emad Mahrous Mohamed and Lin Yan

Abstract—**Due to the slow tracking of acceleration command for pitch autopilot, Robust Servomechanism Linear Quadratic Regulator (RSLQR), three-loop and two-loop autopilot design are driven based on LTI model of missile plant to stabilize the nonminimum phase static unstably missile airframe. Robust Servomechanism Linear Quadratic Regulator (RSLQR) is proposed to design a bank-to-turn (BTT) missile autopilot. Longitudinal autopilot designed using optimal control theory, and is augmented by robust servomechanism design model to further extend the performance and stability of the system. The simulation results using RSLQR approach are compared with two-loop and three-loop designs. The comparison indicated that RSLQR and three-loop topology gives better tracking and more robustly than two-loop with a cascade PI compensator at different value of stability derivative $\mathbf{M_{\alpha}}$.**

Index Terms—**Two-loop autopilot, three-loop autopilot, flight control system, robust servomechanism LQR.**

I. INTRODUCTION

Lateral autopilot acts as an inner loop of the guidance loop which is used to control the pitch and yaw motions. The two- or three-loop autopilots have been introduced in tactical missiles in recent years as in [1], [2]. The pitch autopilots control missiles body by controlling surfaces to track the required acceleration command according to the guidance demand, such as; proportional navigation, augmented proportional navigation, line of sight, etc. In some Russia missile design, one accelerometer and one angular acceleration gyro are used and the accelerometer has to be located in the rear section of the missile for some structure reasons. Nevertheless, the lateral autopilots with one accelerometer and one rate gyro are more commonly used in homing guidance tactical missiles as in [3], [4]. The three-loop Raytheon has been designed especially for radar seeker missile to eliminate the coupling effect of radome and parasitic loop as in [1], [2].

The classical two-loop autopilot consists of rate-damping loop which is used to act as damper and accelerometer loop which provides control of the lateral acceleration of the missile. But when adding a synthetic stability loop, it is called three-loop autopilot as in [5], [6]. When the missile has two planes of symmetry, so we need consider one channel only, the pitch autopilot say. The structured autopilot design algorithm of flight path rate for tactical missile lateral autopilot has been presented as in [7], [8], where the flight dynamic characteristics of the missile depend on its aerodynamic coefficients which vary significantly with flight condition such as altitude and Mach number.

Most industrial flight control problems require a flight control system to accurately track the guidance commands without large dc gains and avoid actuator from saturation due to parameter variations. The characteristics flight dynamic of missile depend on its an aerodynamic stability derivative ($\mathbf{M_{\alpha}}$) which vary significantly with flight conditions such as altitude and Mach number. Literature [9] designed a robustness H_{∞} output feedback controller based on LMI, but it had not considered the aerodynamic stability derivatives variations. So, this work presents a systematic process for building an augmented state space model called the servomechanism design model as in [10], [11]. Which is introduced by creating a new state space model containing the error dynamic and the system model. When the optimal control theory is applied, the state regulation provides accurate tracking of the selected class of the external signals. The goal of the design is to accurately track the normal acceleration command with zero steady-state error without using large dc gains and produces moderate actuator rates without rate saturation for sudden pitch rate demands. This system is decomposed into two parts: a servo tracking controller for command tracking, and a state feedback component for guaranteeing stability. Then the results is compared with the two-loop and three-loop design as in [12].

This paper is organized as in the following. Section II describes the longitudinal autopilot model of a tailed controlled guided homing missile with one accelerometers and one rate gyro whereas the accelerometer is putted coincidence with center of gravity of the missile. Section III presents designing two-loop with a cascade PI controller and three-loop autopilot design. Robust servomechanism LQR (RSLQR) design is given in section IV. Section V presents the performance of the three algorithms. Section VI introduces the conclusion of this work.

II. AUTOPILOT AND MISSILE DYNAMICS

The longitudinal (pitch plane) flight control system for a bank to turn missile form a single input multioutput design model. The autopilot that will be designed will command normal body acceleration using tail fin deflection control. The plant output states are normal acceleration $A_z (ft/s^2)$, and pitch rate q (rad/s), and the plant states are α, q, δ, and $\dot{\delta}$ (angle of attack, pitch rate, fin deflection, and fin rate respectively). The nominal longitudinal airframe dynamics is represented by $G(s)$. The deferential equation used to describe these open loop pitch dynamic as in [13] are:

Manuscript received December 24, 2016; revised February 23, 2017.

The authors are with School of Automation Science and Electrical Engineering, Beihang University BUAA), Beijing 100191, China (e-mail: emadmahrous1977@yahoo.com).

DOI: 10.7763/IJMO.2017.V7.553

$$\left.\begin{aligned}\dot{\alpha} &= Z_\alpha\,\alpha + q + Z_\delta \delta_e \\ \dot{q} &= M_\alpha\,\alpha + M_\delta \delta_e\end{aligned}\right\} \tag{1}$$

$$A_z = VZ_\alpha\,\alpha + VZ_\delta\,\delta \tag{2}$$

Assuming that the actuator is second order system as

$$\ddot{\delta_e} = -2\,\zeta\omega\dot{\delta_e} - \omega^2(\delta_e - \delta_c) \tag{3}$$

In the state space form, the airframe dynamics are represented by the following state space triple $(\mathrm{A}, \mathrm{B}, \mathrm{C})$:

$$\dot{X} = AX + BU \tag{4a}$$

$$Y = CX + DU \tag{4b}$$

where $\mathrm{A} = \begin{bmatrix} Z_\alpha & 1 & Z_\delta & 0 \\ M_\alpha & 0 & M_\delta & 0 \\ 0 & 0 & 0 & 1 \\ 0 & 0 & -\omega^2 & -2\zeta\omega^2 \end{bmatrix}, B = \begin{bmatrix} 0 \\ 0 \\ 0 \\ \omega^2 \end{bmatrix},$

$$C = \begin{bmatrix} VZ_\alpha & 0 & VZ_\delta & 0 \\ 0 & 1 & 0 & 0 \end{bmatrix}.$$

The transfer function matrix is $G(s) = C(sI - A)^{-1}\,\mathrm{B}$. The longitudinal missile dynamics form a single input multioutput design model. From equation 4, the transfer function matrix from the elevon fin deflection command δ_c to the normal acceleration A_z and pitch rate q is

$$\mathrm{G(s)} = \begin{bmatrix} \dfrac{\omega^2 V(Z_\delta s^2 + Z_\alpha M_\delta - Z_\delta M_\alpha)}{(s^2 - Z_\alpha\, s - M_\alpha)(s^2 + 2\zeta\omega\, s + \omega^2)} \\ \dfrac{\omega^2(M_\delta s^2 + M_\alpha Z_\delta - M_\delta Z_\alpha)}{(s^2 - Z_\alpha\, s - M_\alpha)(s^2 + 2\zeta\omega\, s + \omega^2)} \end{bmatrix} = \begin{bmatrix} \dfrac{A_z(s)}{\delta_c(s)} \\ \dfrac{q(s)}{\delta_c(s)} \end{bmatrix} \tag{5}$$

where $Z_\alpha, Z_\delta, M_\alpha, M_\delta$ and M_q are the aerodynamic stability derivatives, and each of them are functions of velocity, dynamic pressures, angle of attack, and center of gravity. The measurements that are available are normal acceleration $A_z = VZ_\alpha\,\alpha + VZ_\delta\,\delta$ (ft/s2), q pitch rate (rad/s). The scalar control input u=δ_c (rad) is the fin angle command. The above aerodynamics have been linearized and represented a trim α angle of attack of 16 degrees, Mach number =0.8, *V*=886.78 (ft/s), an altitude of 4000 (ft.), actuator damping ζ =0.6, and actuator natural frequency ω=113 (rad/s). The following parameters are the nominal values of the dimensional aerodynamic stability derivatives; $Z_\alpha = -1.3046$ (1/s); $Z_\delta = -0.2142$ (1/s); $M_\alpha = \pm 47.7109$ (1/s2) which were taken from [4]. The sign of M_α determines the stability of the open loop airframe. When the M_α is negative the aerodynamic center-of-pressure (cp) is aft of the center-of-gravity (cg) and the airframe is statically stable. This is usually occurs at low angle of attack. While the missile maneuver to higher α, the cp moves forward of the cg creating unstable flight condition. This is indicated by a sign change in M_α from negative to positive [1], [5].

III. Two-Loop And Three-Loop Design

The two-loop autopilot system uses two loops to feedback an information of the missile motion to the forward path of the autopilot. One loop is involved with body rate information through the rate gyro. The other is the missile acceleration feedback measured by accelerometer that considered the main feedback loop. Equation (5) is used to design the normal acceleration command autopilot. In order to eliminate the static error, there are two controller blocks contained in the acceleration command autopilot as shown in the fig.1. The control input is fin deflection command δ_c and the measured outputs are normal acceleration A_z and pitch rate q. The longitudinal autopilot controller blocks $K_{A_z}(s)$ and $K_q(s)$ are designed to give a good acceleration command tracking and to ensure missile stability.

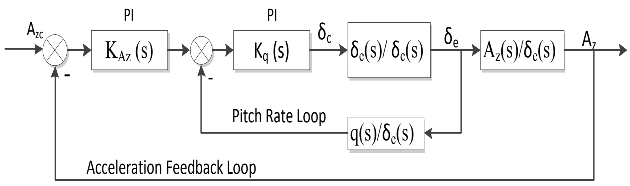

Fig. 1. longitudinal autopilot.

The controller blocks $K_{A_z}(s)$, and $K_q(s)$ consist of proportional-plus-integral (PI) control elements. The acceleration feedback loop controller block $K_{A_z}(s)$ has the structure

$$K_{A_z}(s) = \frac{k_z(s + a_z)}{s}$$

where the k_z is the proportional gain, and $k_z a_z$ is the integral control gain. The pitch rate loop controller block $K_q(s)$ has the structure

$$K_q(s) = \frac{k_q(s + a_q)}{s}$$

The feedback gains of the two-loop autopilot as got as in [12] are $k_q = -0.3$, $k_z = -0.00$, $a_q = 6$, $a_z = 2$, and $a_z = 2$.

The two-loop autopilot is modified with a new kind of autopilot developed recently years by adding one feedback loop (it is called synthetic loop). Also a pure integrator is contained in the forward path of the autopilot loop. The three-loop pitch/yaw autopilot is used to most guided tactical missiles today as shown in Fig. 2. It has four gains K_{DC}, K_A, K_R, and ω_I; which are used to control the fourth order dynamics of the autopilot. These dynamics are due to second order dynamics and an integrator that allows the flight control system to control unstable airframe.

The performance values examined are the normal acceleration command settling time, the steady state error the percent undershoot and overshoot. It found that the three-loop autopilot feedback gains are $k_{DC} = 1.061$, $k_A = -0.007$, $\omega_I = 18.8$, $k_R = -0.7$. The contribution of the controller blocks $K_{A_z}(s)$, and $K_q(s)$ of the two-loop design and three-loop are compared with RSLQR algorithm in Section V.

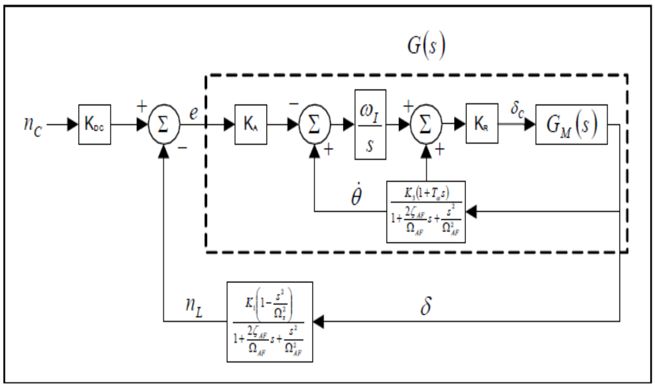

Fig. 2. Standard three-loop autopilot as in [14].

IV. Robust Servomechanism LQR

It is desired to design an autopilot to track the required acceleration command $r = A_z$ that is coming from the guidance loop. The autopilot will be designed using an RSLQR approach as shown as in fig.3. The goal is to drive the error $e_r = y_c - r$ to zero, this forces the normal acceleration to track the command input r, which it is assumed constant. We design a constant gain matrix K_c for a single flight condition which it is available, and will assume that gain scheduling will be used to interpolate the gains between other design points.

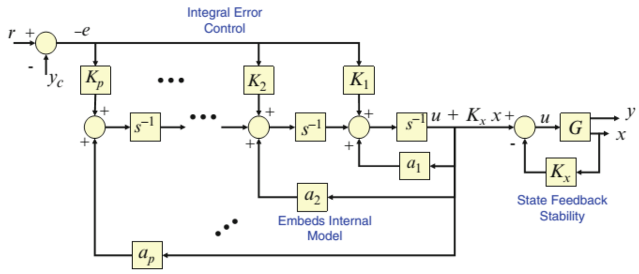

Fig. 3. Robust servomechanism block diagram.

We can introduce A_z directly in (2) as a state variable by replacing the angle of attack α. Differentiate (2) to produce the differential state for $\dot{A}_z$ and then substitute for $\dot{\alpha}$ from (1). This produces

$$\begin{cases} \dot{A}_z = Z_\alpha A_z + VZ_\alpha\, q + VZ_\delta \dot{\delta}_e \\ \dot{q} = \frac{M_\alpha}{VZ_\alpha} A_z + \left(M_\delta - \frac{M_\alpha Z_\delta}{Z_\alpha}\right) \delta_e \end{cases} \tag{6}$$

Since $r = constant, \dot{r} = 0, and\ p = 1$, so it needs to add an integrator to form a type 1 controller. This will form a controller that achieves zero steady-state error to a constant command. The servomechanism design model is represented by creating a new state space model, containing the error dynamic and the system model. The new state vector is z defined as

$$z = \left[e\ \dot{e} \ldots\ e^{(p-1)}\ \ e\ \ \xi\right]^T \tag{7}$$

This new state vector z has dimension $(n_x + p \times n_r)$. Differentiating (7) yields the robust servomechanism design model:

$$\dot{z} = \tilde{A}z + \tilde{B}\mu \tag{8}$$

The state vector of (8) for the robust servomechanism design model is

$$\dot{z} = [e \quad \dot{x}^T]^T \tag{9}$$

with the design model $\dot{z} = \tilde{A}z + \tilde{B}\mu$ given as:

$$\begin{bmatrix} \dot{e} \\ \ddot{A}_z \\ \ddot{q} \\ \ddot{\delta}_e \\ \dddot{\delta}_e \end{bmatrix} = \begin{bmatrix} 0 & 1 & 0 & 0 & 0 \\ 0 & Z_\alpha & VZ_\alpha & 0 & VZ_\delta \\ 0 & M_\alpha/VZ_\alpha & 0 & (M_\delta - M_\alpha Z_\delta/Z_\alpha) & 0 \\ 0 & 0 & 0 & 0 & 1 \\ 0 & 0 & 0 & -\omega^2 & -2\zeta\omega \end{bmatrix} \begin{bmatrix} e \\ \dot{A}_z \\ \dot{q} \\ \dot{\delta}_e \\ \ddot{\delta}_e \end{bmatrix} + \begin{bmatrix} 0 \\ 0 \\ 0 \\ 0 \\ \omega^2 \end{bmatrix} \dot{\delta}_c \tag{10}$$

where $\dot{z} = [e \quad \dot{A}_z \quad \dot{q} \quad \dot{\delta}_e \quad \ddot{\delta}_e]^T \in R^5$.

The objective of the design is to track the normal acceleration command with zero steady state error without using large gains. The design begins by equating R = 1 and select a Q matrix which penalize the error state e in (10). So the performance index will be

$$J = \int_0^\infty (z^T Q z + \mu^T \mu)\, d\tau \tag{11}$$

We start by selecting the parameter of q_{11} in the (1,1) element of $z^T Q z$, and set the other matrix elements to zero. This penalize the error in the command signal as in (30).

$$z^T Q z = z^T \begin{bmatrix} q_{11} & 0 & 0 & 0 & 0 \\ 0 & 0 & 0 & 0 & 0 \\ 0 & 0 & 0 & 0 & 0 \\ 0 & 0 & 0 & 0 & 0 \\ 0 & 0 & 0 & 0 & 0 \end{bmatrix} \begin{bmatrix} e \\ \dot{A}_z \\ \dot{q} \\ \dot{\delta}_e \\ \ddot{\delta}_e \end{bmatrix} \tag{12}$$

Substituting (12) into (11) gives the performance index as

$$J = \int_0^\infty (\, q_{11} e^2 + \mu^2)\, d\tau \tag{13}$$

If we check the controllability and observability of the augmented system, we find that (a) the pair $(\tilde{A}, \tilde{B})$ is controllable to guarantee that the unstable mode of (2) are controllable with the input vector; (b) $Q \geq 0, R > 0$, all are symmetric to provide a sufficient conditions for the solution of the Algebric Raccatti Equation (ARE); and (c) the pair $(\tilde{A}, Q^{1/2})$ is observable through this choice of Q as in (30) to guarantee stability of the closed-loop system using the state feedback control structure:

$$\text{ARE: } P\tilde{A} + \tilde{A}^T P - P\tilde{B}R^{-1}\tilde{B}^T + Q = 0 \tag{14}$$

$$K_c = R^{-1}\tilde{B}^T P \tag{15}$$

$$\mu = -K_c x \tag{16}$$

By using the feedback gain matrix computed in (15) the closed loop is given by

$$\dot{z} = \left(\tilde{A} - \tilde{B}K_c\right)x = \tilde{A}_{cl}x + Fr \tag{17}$$

where $F = [-I_{n_u \times n_u} \quad 0_{n_u \times n_u}]^T$.

The computation steps are the following:

1) Set value of q_{11} in Q form (12).
2) Solve the ARE in the (14) for find P.
3) Compute the feedback gain matrix K_c in (15)
4) Form the closed loop system in (17).

For the flight conditions mentioned in section II, a suitable value of q_{11} was selected, when the percent overshoot first approaches to zero. This produces the state feedback gain matrix $K_c = [0.4948\ 0.0491\ -2.7132\ 11.1850\ \ 0.0095]$ for $M_\alpha = 47.7109\ (1/s^2)$; and all poles of the closed loop system locate at right half plane (RHP). Then simulate the closed loop system to a step command. the states A_z, q, δ_e, and $\dot{\delta}_e$ are plotted versus time as in fig. 4, 5, 6, and 7 at different values of an aerodynamic stability derivative M_α for the same state feedback gain matrix K_c.

V. Simulation And Analysis

To evaluate the control system design, a step simulation of the closed loop system was performed. The speed of the response is measured using the 63% rise time, which is approximate the time constant. The command overshoot and the damping in the response is measured by 95% settling time. The smaller rise time (time constant), the faster response are achieved as shown in Fig. 4.

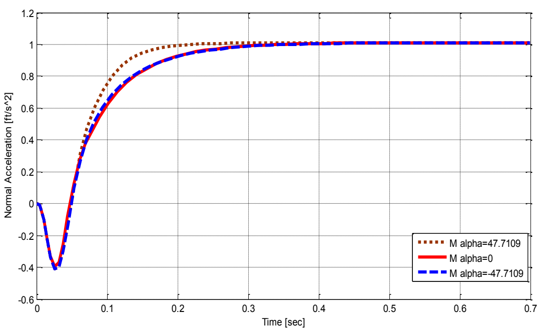

Fig. 4. Unit step response history of normal acceleration.

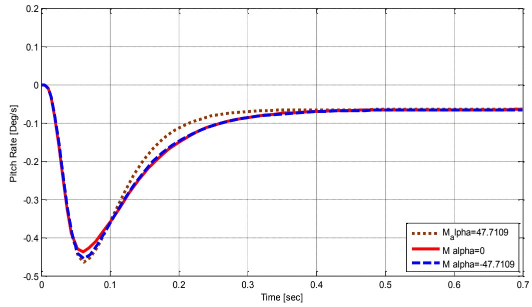

Fig. 5. Unit Step response history of pitch rate.

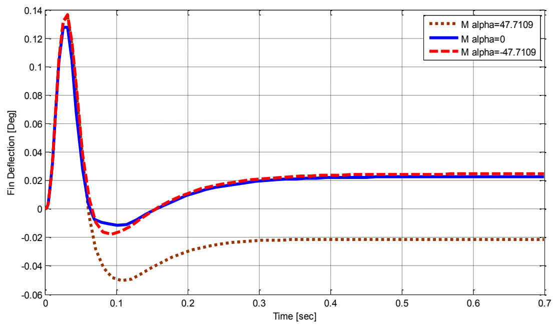

Fig. 6. Unit Step response history of fin deflection.

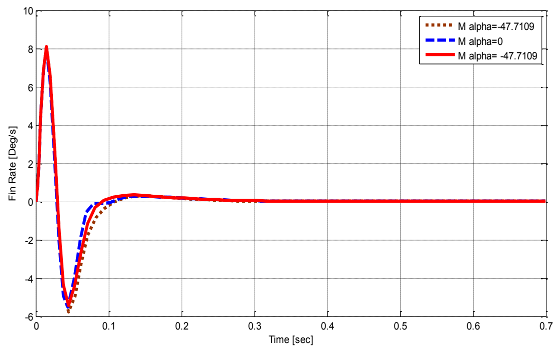

Fig. 7. Unit Step response history of fin deflection rate.

Firstly, It is shown from the simulation results Fig. 4 that the small rise time and settling time with no overshoot which indicate damping and quick response that accurately track the input command and a very small change with different value of M_α without using large dc gains. Where $K_c = [0.4948\ 0.0491\ -2.7132\ 11.1850\ 0.0095]$ is the same for stable and unstable modes what it can be implemented in the practice. Secondly, it is seen from Fig. 5 and 7 that the actuator responding to the control signal is not positioned or rate saturated. However, a right-half-plane (RHP) zero is initially produces a lift force in the direction opposite to the input command. This force creates a moment causes the airframe to pitch. This phenomena is observed as an initial undershoot in the time history of normal acceleration shown in fig. 4, because the initial value of step response is

$$\lim_{s\to\infty} s\left[\frac{1}{s}\frac{A_z(s)}{\delta_e(s)}\right] = Z_\delta < 0$$

But the final value of the step response is

$$\lim_{s\to 0} s\left[\frac{1}{s}\frac{A_z(s)}{\delta_e(s)}\right] = \frac{Z_\alpha M_\delta - M_\alpha Z_\delta}{-M_\alpha} > 0$$

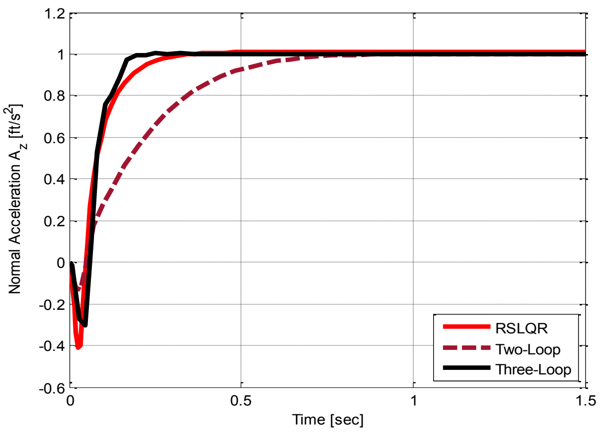

Fig. 8. Unit step response history of normal acceleration.

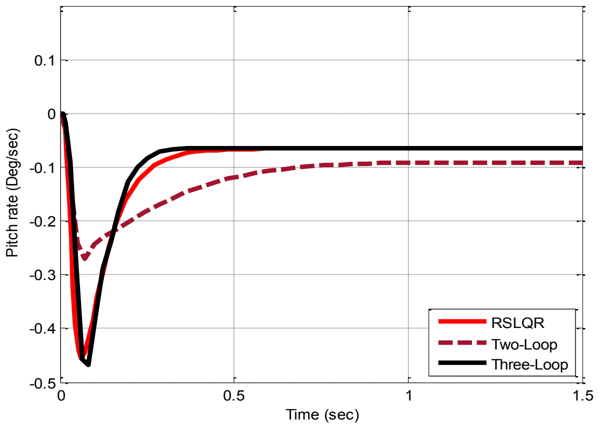

Fig. 9. Unit Step response history of pitch rate

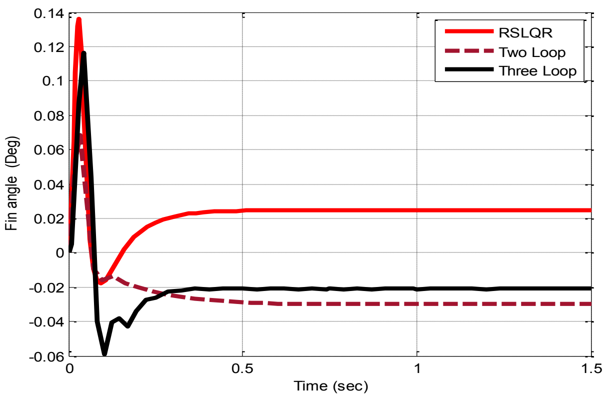

Fig. 10. Unit Step response history of fin deflection.

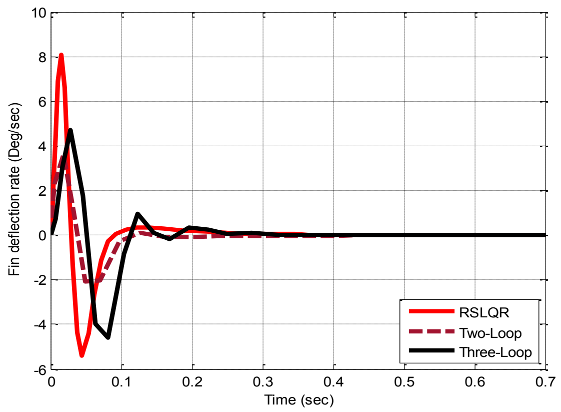

Fig. 11. Unit Step response history of fin deflection rate.

Finally, the RSLQR design results are compared with the two-loop and three-loop autopilot design in case of unstable mode which it is occurred when $M_\alpha = 47.7109$ as shown in Figs. 8, 9, 10 and 11. It can see that the controller design using RSLQR and three-loop give approximately similar results, and better than the two-loop topology except three-loop gives smaller fin angle, fin angle rate, and initial undershoot than RSLQR. Two-loop is slower than RSLQR and three-loop in tracking but it has the smallest fin angle, fin angle rate, and initial undershoot as shown in the Table I. The resulting control architecture of RSLQR provided accurate external command tracking and a robust flight control design with predictable and robust performance but it has a larger initially undershoot than others.

TABLE I: AUTOPILOT DESIGN COMPARISON

	T_r(s)	T_s(s)	Initial U.S(%)	O.S(%)	Max δ (d/s)	Max.$\dot{\delta}$ (d/s)
Two-loop	0.32	0.6	-10	3	0.07	3.5
Three-loop	0.1	0.15	-30	0	0.108	5
RSLQR	0.1	0.2	-40	0	0.14	8.2

Note: T_r is the Rise time , T_s is the Settling Time, O.S is the Overshoot and U.S is the undershoot.

VI. CONCLUSION

RSLQR and three-loop topology are better than two-loop for tracking normal acceleration command. However two-loop with a cascade PI controller has a two advantages better than the others as follows: the first one is the fin deflection and the undershoot percentage have half values compared to others at different values of stability derivative (M_α) which it's sign indicates the stability of the airframe. The last one is it has the smallest value of the fin rate, and pitch rate which could produce moderate actuator rates without rate saturation for sudden pitch rate demands. The robust servomechanism LQR (RSLQR) closed loop design using state feedback is easy to implement in practice due to its small state feedback gains K_c, and is guaranteed to be globally exponential stable. It forces the system regulated output tracks quickly the selected normal acceleration command without overshoot and with zero steady state error. In addition, it drives the control surface actuator without large gains that cause large actuator deflections and deflection rates, which are not desirable. Finally three-loop has smaller undershoot than RSLQR, but RSLQR is easy to implement in practice due to its small state feedback gains K_c, and is guaranteed to be globally exponential stable.

REFERENCES

[1] P. Zarchan, "Tactical and strategic missile guidance," in *Proc. 4th Edition*, Virginia: AIAA Inc, 2002, 70-73.
[2] E. Devaud, H. Siguerddidjane, and S. Font, *Control Engineering Practice*, pp. 885-892, 2000.
[3] P. Garnel, *Guided Weapon Control Systems*, 2003.
[4] E. Devaud, H. Siguerddidjane, and S. Font, *Control Engineering Practice*, 2001.
[5] F. W. Nesline and M. L. Nesline, "How Autopilot Requirements constrain the aerodynamic design of homing missiles," in *Proc. Conference Volume of 1984 American Control Conference*, San Diego, CA, June 6-8, 1984.
[6] F. Lun-fang, C. Ying, and L. Peng, "Control analysis for a non-minimum phase static unstably missile," in *Proc. 14th International Conference on Control, Automation and Systems*, Oyeonggi-do, Korea, Oct. 2014.

[7] G. Das, K. Datta, T. K. Ghoshal, and S. K. Goswami, "Structured designed methodology of missile autopilot," *Journal of the Institution of Engineers (India)*, pp. 49-59.
[8] G. Das, K. Datta, T. K. Ghoshal, andS. K. Goswami, "Structured designed methodology of missile autopilot- II," *Journal of the Institution of Engineers (India)*, pp. 28-34.
[9] G. Quanying and S. Jianmei, "Design of missile's attitude tracking controller based on H robust output feedback Acta Aramamentarii," 2007.
[10] B. A. Francis and W. M. Wonham,, "The internal model principle of control theory," *Automatica*, vol. 12, no. 5, pp. 457–465, 1976.
[11] E. J. Davidson and B. Copeland, "Gain margin and time lag tolerance constraints applied to the stabilization problem and robust servomechanism problem, " *IEEE Transactions on Automatic Control*, 1985.
[12] E. Mohamedand L. Yan, "Design and comparison of two-loop with PI and three-loop autopilot for static unstable missile," *International Journal of Computer and Electrical Engineering*, vol. 8, no. 1, February 2016.
[13] K. A. Wise and R. Eberhardt, "Automated gain schedules for missile autopilots using robustness theory," in *Proc. of the First IEEE Conference on Control Applications*, Dayton, OH, May, 1992.
[14] Z. Paul, "Tactical and strategic missile guidance," *Progress in Astronautics and Aeronautics*, vol. 176, Virginia, 1997.

Emad Mahrous Rabie Mohamed was born in 1977. He received his B.S degree in electrical power engineering from Military Technical College, Cairo, Egypt in 2002 and the M.S. degree in control system from Cairo University, Egypt in 2009. He is currently a Ph.D. student in the Department of Automatic Control, School of Automation Science and Electrical Engineering, Beihang University BUAA), Beijing, China. He started in 2014 for his Ph.D. degree. His main research interest is missile guidance and control systems.

Yan Lin was born in 1955. He received the M.S. and Ph.D. degrees from Beihang University (BUAA), in 1988 and 1999, respectively. He is currently a professor in the School of Automation, BUAA. His research interests include robust control and adaptive control. Prof. Lin is in charge of National Natural Science Foundation of China, Doctoral Fund, Beijing Natural Science Foundation and sub-topic of 863 project, and participates in project of Beijing key Discipline Foundation. As a major participant of National Natural Science Foundation of China, he won the second prize of 1998 Science and Technology Progress Award of Aviation Industry Corporation. He is a coauthor of more than 50 papers published in the IEEE and other international journals.